Control of the ionization state of three single donor atoms in silicon

B. Voisin, M. Cobian, X. Jehl, M. Vinet, Yann-Michel Niquet, Christophe Delerue, Silvano de Franceschi, M. Sanquer

PHYSICAL REVIEW B **89**, 161404(R) (2014)

Control of the ionization state of three single donor atoms in silicon

B. Voisin,[1] M. Cobian,[2] X. Jehl,[1] M. Vinet,[3] Y.-M. Niquet,[2] C. Delerue,[4] S. de Franceschi,[1] and M. Sanquer[1,*]

[1]*SPSMS, UMR-E CEA/UJF-Grenoble 1, INAC, 17 rue des Martyrs, 38054 Grenoble, France*

[2]*SPMM, UMR-E CEA/UJF-Grenoble 1, INAC, 17 rue des Martyrs, 38054 Grenoble, France*

[3]*CEA, LETI, MINATEC Campus, 17 rue des Martyrs, 38054 Grenoble, France*

[4]*IEMN, 41 Boulevard Vauban, 59046 Lille, France*

(Received 6 December 2013; published 16 April 2014)

By varying the front-gate and the substrate voltages in a short silicon-on-insulator trigate field-effect transistor, we control the ionization state of three arsenic donors. We obtain good quantitative agreement between three-dimensional electrostatic simulations and experiment for the control voltages at which the ionization takes place. It allows us to observe the three doubly occupied states As^- at strong electric field in the presence of nearby source-drain electrodes.

DOI: 10.1103/PhysRevB.89.161404 PACS number(s): 73.22.Dj, 73.23.Hk, 73.63.−b

Semiconducting devices have entered a new era where single dopants can be used for new (quantum) functionalities [1,2]. Thin silicon-on-insulator (SOI) devices are particularly attractive in this perspective, offering good control of the transverse electric field in the channel. This electrostatic property, at the core of the metal-oxide-semiconductor field-effect transistors (MOSFETs), is crucial to address dopants individually and to control their electronic wave functions and couplings. These are prerequisites for dopant-based applications.

In this work we study, both experimentally and with simulations, how three arsenic donors are charged in a nanoscopic MOSFET. The ionization state of each donor is separately read out by detecting its corresponding resonance in the source-drain (S-D) current. The ionization state of each donor—As^+, As^0 or As^-—is individually controlled at low temperature by tuning the transverse electric field with a front and a back gate. The scalability of a compact system of a few tunable shallow donors beyond the previously studied cases of one [3–7] and two donors [4,8] is then shown.

In our small MOSFETs—in the 10 nm size range—dopants are not isolated in the channel but see a complex electrostatic environment which should be considered cautiously. It includes other donors in the channel and in the heavily doped S-D leads, as well as offset charges in the gate stack. First the interaction among donors, which may result in a Coulomb glass [9], is screened by the S-D leads [see the inset of Fig. 1(c) which shows a weak interaction between two donors]. Therefore we can independently address the gate-induced charge transitions of a given donor while assuming the other donors to be in a constant ionization state. Secondly, the ionization of donors at the graded edges of the S-D leads—which we shall refer to as lead extensions—is explicitly considered in our simulation in a mean-field approach, neglecting Kondo [10] and Fermi edge singularity [11] effects, which are not observed in our devices at 4.2 K. The simulation of a realistic electrostatic environment explains the evolution of the donor ionization lines (DIL) as a function of the control voltages.

The samples, fabricated on 200 mm SOI wafers, are similar to those described in Ref. [3]. A 200-nm-long, 17-nm-thick, and 50-nm-wide silicon nanowire was etched from the SOI film and covered at its center by a 30-nm-long polysilicon gate isolated by a 4-nm-thick SiO_2 layer, called the front oxide (FOX) [see Figs. 1(a), 1(b)]. This front gate covers three sides of the silicon channel in a so-called trigate geometry. A 400-nm-thick buried oxide (BOX) separates the channel from the silicon substrate, which can be biased using the procedure described in Ref. [12]. The central part of the channel contains a few arsenic donors as estimated by process simulations including the rapid thermal annealing step for donors activation [3]. The device differential conductance (G) was measured at $T = 4.2$ K using standard lock-in detection. The extensions of the S-D are located below the gate because there are no spacers. Therefore the channel length (between 10 and 20 nm) is significantly smaller than the nominal gate length (30 nm) [3], resulting in the donors centered in the channel to have sufficient tunnel couplings to S-D and therefore to be detected by resonant tunneling.

Figure 1(c) shows a color plot of G as a function of substrate voltage V_b and front gate voltage V_g at a dc S-D bias $V_d = 0$. Above a certain threshold voltage the S-D current has contributions coming from the continuum of delocalized conduction-band states. The donors in the body of the SOI contribute below this threshold, giving rise to resonant tunneling conduction paths whenever their energy levels lie in the bias window [3]. At $V_b = 0$, the channel conduction starts at $V_g \simeq 0$–0.1 V, which is the expected threshold voltage for the gate stack used [13]. $V_b \simeq V_g \simeq 0$ corresponds to the flat-band regime without evidence for donor states. At $V_b > 0$, conduction starts at negative V_g, and a large transverse electric field is present in the channel. Carriers are accumulated at the BOX interface and the threshold shows a kink in the (V_b, V_g) plane [see the blue dashed line in Fig. 1(c)]. In the case of P-doped, macroscopic SOI films, this kink has been attributed to the ionization of donors in the body of the channel when a vertical electric field is applied [14]. In the middle of a long undoped channel the kink is due to the shift of the two-dimensional electron gas (2DEG) from the top to the back-gate interface [15]. It is different in our short nanoscale field-effect transistor where the S-D leads end up with a strong gradient of As atoms near the channel. In these S-D extensions the carrier density and the ionization state of the donors can change with V_g and V_b. This affects the potential landscape in

*marc.sanquer@cea.fr

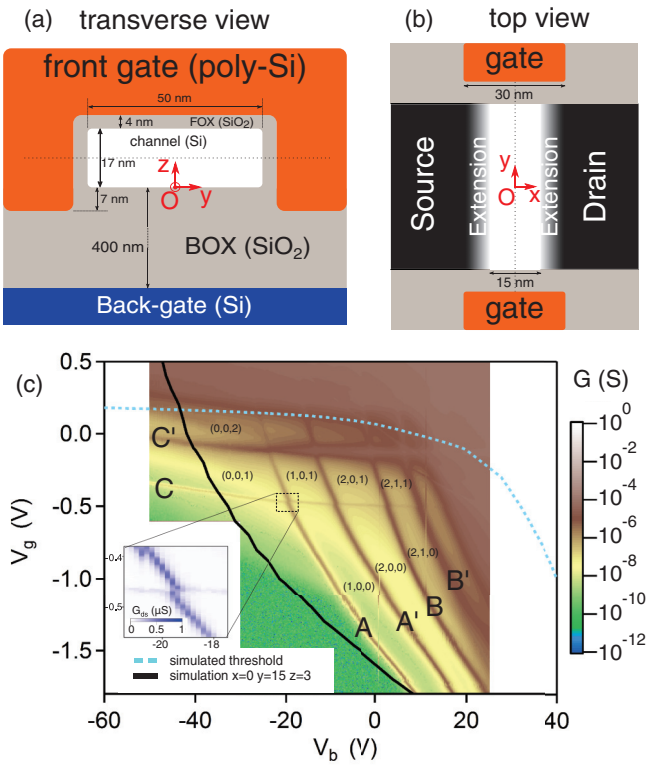

FIG. 1. (Color online) (a),(b) Schematic cross-sectional view of the device. Vertical cut along the transverse z-y plane (a) and horizontal cut along the x-y plane (b). (c) Color plot of the source-drain linear conductance vs back- and front-gate voltages (V_b and V_g, respectively) at $T = 4.2$ K. The blue dashed line is the simulated threshold voltage assailing no donors in the channel. The three pairs of DILs, denoted by A-A', B-B', and C-C', are found in the subthreshold regime. They correspond to the As^+/As^0 and As^0/As^- transitions of three As donors. The ionization states (a,b,c) for the three donors are indicated between the DILs (a, b, and c can be 0, 1, or 2 depending on whether the corresponding donor is empty, singly, or doubly occupied, respectively). States with more than four electrons on the three donors are barely visible because of the strong coupling with the conduction band. According to our simulation the donor corresponding to the C-C' pair of DILs is closer to the front gate, while the other two donors are closer to the BOX. The black line is the simulated DIL for a donor located at $(x,y,z) = (0,$ 15, and 3 nm). Inset: Zoom-in of the crossing between the A and C DIL at $T = 1$ K showing a weak Coulomb repulsion.

the whole channel and the curvature of the threshold line [16]. As we shall show below, the response of the donors and conduction electrons in the S-D extensions affects the slope and position of both the threshold voltage line and the DILs.

We have simulated the DIL of a few donors in the channel of our trigate transistor. For that purpose, we have treated the few donors in the channel as interacting point charges, and the donors in the highly doped source and drain extensions as a continuum. We have first computed the potential landscape $V(\vec{r})$ in the nanowire channel at $V_d = 0$ [16]. To this aim, we have solved Poisson's equation self-consistently using the Fermi integral $F_{1/2}(\frac{E_c - eV(\vec{r}) - \mu}{k_B T})$ as an approximation for the local density of electrons. The density of ionized donors in the S-D extensions is approximated as in Ref. [17]. Here E_c and μ are the silicon conduction-band edge and the device chemical potential, respectively. The ∼15-nm-long channel was left undoped, and the simulations were run at 30 K for computational reasons. This simple model shall give a fair account of the screening by the quasimetallic S-D extensions. It provides, admittedly, a coarse description of the channel, but our interest here is the physics of individual donors, thus below the channel threshold. Once the potential landscape has been computed as a function of V_b and V_g, we have added a few bulklike donors in the channel at positions $\vec{r}_i$, and have tracked their bound-state energy levels $E_{1s}(V_b,V_g,\vec{r}_i) = E_c - E_b - eV(\vec{r}_i)$ (where E_b is the binding energy of these donors, 53 meV). We have also computed the Coulomb interactions U_{ij} between these donors as the screened Coulomb interactions between point charges. We have finally used these data as input for a Coulomb-blockade-like model of the donor system in order to determine the DIL of each donor.

First of all, we have computed the threshold voltage as the voltage where the electron concentration, integrated over the SOI thickness, exceeds 10^{11} cm^{-2} [in the (V_b,V_g) plane of Fig. 1(c), this threshold is denoted by a blue dashed line]. The kink near $V_b \simeq V_g \simeq 0$ and the absolute values for V_b and V_g are in excellent agreement with the experimental data. We start with one single donor located at $(x = 0,\ y = 15,\ z = 3)$ nm [see Figs. 1(a), 1(b) for a definition of the spatial coordinates; in our reference, $(x = 0,\ y = 0,\ z = 8.5)$ corresponds to the center of the channel, $|x| \geqslant 7.5$ nm are the S-D extensions]. The $(x = 0,\ y = 15,\ z = 3)$ nm position is chosen such that it approximately corresponds to the experimental DIL for dopant A (Fig. 1(c), black solid line). The DIL is curved in the (V_b,V_g) plane, which cannot be captured with a model assuming perfectly metallic S-D leads and constant capacitive couplings between the donor and all the surrounding electrodes (such would yield only straight DILs). The curvature indicates that the couplings to the gate and substrate evolve with V_b and V_g, as a result of the ionization of donors in the extensions and of the accumulation of surface carriers. Taking this complex electrostatic environment into account is necessary to reproduce the DILs in the channel. In particular the DIL become less dependent on V_g, when V_b is decreased. The donor's ionization thus occurs at higher V_g values where the conduction channel is set in the extensions of S-D. The latter screens the gate potential at the bottom of the channel, therefore on the donor site.

In Fig. 2 we introduced two more donors whose positions differ either in x, y, or z. A change in x [with constant y,z, see Fig. 2(a)] produces three almost parallel DIL. This is because the lever arm parameters change ($\alpha_g = \frac{\delta\phi}{\delta V_g}$, $\alpha_b = \frac{\delta\phi}{\delta V_b}$, where ϕ is the electrostatic potential at the donor position). A donor centered in the channel has larger lever arm parameters (which means a better electrostatic control by V_b and V_g) than a donor located closer to the S-D extensions. In other words, there is a significant electric field along x in our structure when finite V_g and V_b are applied. The parallelism between the 3 DIL suggests that the ratio of $\frac{\alpha_g}{\alpha_b}$ is barely affected. As a result donors close to the S-D ($|x| \simeq 5$) are charged (As^+ to As^0) at the largest negative V_g values. Donors more centered in the channel ($|x| \simeq 0$ or 3) are still ionized at this value of V_g thanks to the potential gradient along x.

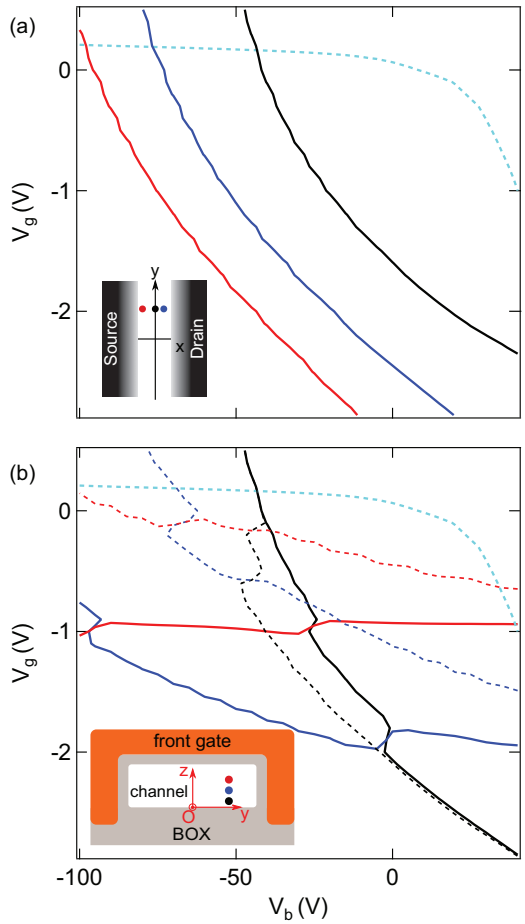

FIG. 2. (Color online) Calculated DILs in the (V_b, V_g) plane for a three-donor configuration. (a) The donors differ by their x position ($x, y = 15$ nm, $z = 3$ nm) as sketched in the inset: $x = 0$ (respectively, 3, -5) for the donor represented in black (respectively, blue, red), keeping a constant distance to the gates. (b) The donors differ by their z [$(x = 0,\ y = 15,\ z = \{3$ (black), 7.5 (blue), 12 (red)$\}$), full lines], as sketched in the inset, or y [$(x = 0,\ y = \{15$ (black), 20 (blue), 23 (red)$\},\ z = 3$), dashed lines] position. Both cases correspond to varying the distance to the front gate. For all simulations, the black donor is at the same position as the simulated one in Fig. 1(c).

On the contrary a change in y or in z [see Fig. 2(b)] modifies the distance between the donor and the gates, which very much influences the DIL's curvature, i.e., $\frac{\alpha_g}{\alpha_b}$. Donors located at the bottom center of the channel (near the BOX) are charged first at $V_b \gg 0$ and $V_g \ll 0$. Donors closer to the front gate (large y or large z) are charged first at positive V_g and they are less sensitive to V_b, like the DIL C-C' in Fig. 1(c). Therefore, a measurement of the DILs as function of V_b and V_g [i.e., the A-A', B-B', and C-C' DILs in Fig. 1(c)] allows one to deduce the position of the corresponding donors [18] (i.e., donors A, B, and C, respectively) relative to the FOX and the BOX [see Fig. 1(a)].

Remarkably, A-A', B-B', and C-C' in Fig. 1(c) form three pairs of approximately parallel DILs, each pair being associated with a different donor (i.e., A, B, and C, respectively). We attribute the upper line of each pair to the loading of the doubly occupied donor state (i.e., the As^0/As^- transition). The distance between this upper line and the corresponding lower line is set by the intradonor charging energy. The fact that the DILs of a given pair are parallel to each other indicates that the intradot charging energy does not depend on the electric field in the channel. The positions and the slopes of the A-A' and B-B' DILs indicate two donors near the BOX and approximately centered in the channel (i.e., small y and z). By contrast the C-C' DILs must originate from a donor close to the front gate [large y or z, like the red lines in Fig. 2(b)]. We cannot take into account the double occupation problem in the simulation yet, as it would deserve to include electron-electron interactions beyond the mean-field treatment used here. The strong electric field in the channel, combined with the small number of donors, also favors the population of the As^- state of a donor (e.g., A') rather than the loading the As^0 state of another donor (e.g., B).

Studies at finite bias V_d (see, e.g., Fig. 3) provide a direct measurement of the charging energy E_c and the lever-arm parameter α_g of a given donor (donor A in the case of Fig. 3). We find $E_c \simeq 30$ and 20 meV for donors A and B, respectively. In the case of donor C, we can only estimate a lower bound $E_c \geqslant 30$ meV due to the lack of contrast of the second resonance (As^0/As^- transition), which occurs too close to the threshold (not shown). The lever-arm parameter is smaller for A' ($\alpha_g^{A'} = 0.08$) than for A ($\alpha_G^{A} = 0.12$), i.e., As^- is more strongly coupled to S-D than As^0. Two physical mechanisms account for this observation. First, the As^- electronic orbital is less localized on the donor. Secondly, the ionization of As^- occurs at higher V_g where the S-D are more extended towards the donor. These two mechanisms increase the capacitive couplings to the S-D leads with respect to the capacitive couplings to the gates, resulting in a lower α_g. In addition, the As^- state has a stronger tunnel coupling to the S-D leads. The G lines parallel to Coulomb-diamond edges (clearly visible in Fig. 3) are due to local density-of-states fluctuations in the S-D extensions [3]. The similar pattern for A and A'

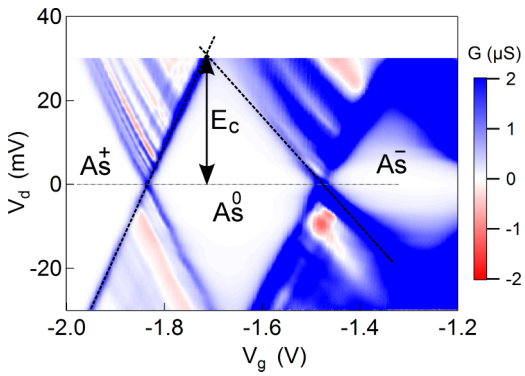

FIG. 3. (Color online) Color plot of the S-D differential conductance at $T = 4.2$ K and $V_b = 10$ V. The observed resonances correspond to DILs A and A'. The Coulomb-blockade regimes associated with the As^+, As^0, and As^- charge states are indicated. As expected, the lever arm factor is smaller for A' than for A (see text). The lines of differential conductance appearing at finite V_d and parallel to the diamond are due to fluctuations in the local density of states of the S-D extensions [3]. They present approximately the same pattern for A and A', but they are more blurred for A' due to the larger tunnel coupling.

(only smoothed for A' due to higher tunneling rates) supports the assumption that A and A' are different ionization states associated with the same donor, feeling the same local environment in the S-D.

Several conclusions can be drawn from our observations. The doubly charged state exists for the three donors. Then, if the charging energy depends on the actual donor position and consequently on its mesoscopic environment [19,20], the measured E_c are much smaller than the ionization energy for As donors in bulk ($\simeq$53 meV) and the double occupied states are well separated from the conduction-band threshold. Hence the double occupied state of a donor is more stable in our nanostructure than in the bulk case. Finally, E_c does not depend significantly on the electric field in the channel. In previous experiments [20] the electric field could not be varied on demand.

The stability of the doubly occupied state of shallow donors in the presence of an interface has been the subject of intense research [21–23]. The reduction of E_c can be due to the screening by a metallic gate electrode separated from the silicon by a very thin dielectric barrier [15,22,23], or to the electric-field-induced hybridization of the donor state with a conduction-band state at Si/SiO_2 interface [20]. In particular, our calculations give $E_c \simeq$ 20–30 meV for donors located 3–5 nm from the interface in the presence of a strong transverse electric field of $\sim$30 mV/nm, which is in good quantitative agreement with our experimental results. The fact that E_c does not depend on the electric field indicates that the electric field is always large in our device (which is in agreement with our simulation), such that donors lying close to the BOX or to the FOX are strongly hybridized with an interfacial state. As opposed to the previous works mentioned above, here we have shown that the S-D leads have an important screening role leading to a reduced E_c in our devices [24]. Moreover, the predicted binding energy for the doubly occupied state remains small with or without the gate.

The charging sequence of the hybrid state could be the following. An As ion located a few nanometers away from an interface in the bulk is always ionized at large electric fields. It creates a local positive potential which forms a donor-induced potential dip at the interface. This dip attracts an electron and forms the singly occupied state As^0. It is important to note that the first electron does not fully screen the As^+ ion but rather forms a dielectric dipole with it (transverse to x). This dipole produces a local field which is larger than the screened central potential which would result from the singly occupied neutral state in the absence of electric field. The doubly occupied state As^- could be stabilized in that situation even if it is hard to conclude definitely on this point as it involves complex correlation effects between the two electrons and their image charges at the interfaces. This scenario may explain why the lines A and A' run parallel to the conduction-band edge at large positive V_b, because the interface 2DEG and the Coulomb island induced by the ionized donor potential have exactly the same coupling to the substrate and to the front gate. Both effects—the shift of the electron from the donor under large transverse electric field (along y,z) and the screening by the S-D electrodes (along x)—can help to explain the reduction of the charging energy and the stabilization of the As^- state. However, a full simulation of the two-electron problem is lacking for a more quantitative analysis.

In summary we have tuned independently the ionization state of three randomly implanted As donors in a nanoscale silicon MOSFET channel at low temperature, by applying both a front-gate and a back-gate voltage. We have shown the dominant screening role of the S-D leads, which combined with the existence of hybridized states due to the large transverse electric fields, results in a stabilization of the donor doubly occupied state with a decreased charging energy compared to the bulk case. This understanding of the complex environment around a dopant is essential for the perspectives of donor-based quantum applications.

We thank B. Sklenard and O. Cueto for extensive process simulation. The authors acknowledge financial support from the EU, through the EC FP7 MINECC initiative under Project TOLOP No. 318397 and through the ERC Grant Agreement No. 280043, and from the French ANR, through the project SIMPSSON No. 2010-Blan-1015.

[1] F. A. Zwanenburg, A. S. Dzurak, A. Morello, M. Y. Simmons, L. C. L. Hollenberg, G. Klimeck, S. Rogge, S. N. Coppersmith, and M. A. Eriksson, Rev. Mod. Phys. **85**, 961 (2013).

[2] B. Roche, R.-P. Riwar, B. Voisin, E. Dupont-Ferrier, R. Wacquez, M. Vinet, M. Sanquer, J. Splettstoesser, and X. Jehl, Nat. Commun. **4**, 1581 (2013).

[3] M. Pierre, R. Wacquez, X. Jehl, M. Sanquer, M. Vinet, and O. Cueto, Nat. Nanotechnol. **5**, 133 (2010).

[4] M. A. H. Khalafalla, Y. Ono, K. Nishiguchi, and A. Fujiwara, Appl. Phys. Lett. **91**, 263513 (2007).

[5] M. A. H. Khalafalla, Y. Ono, K. Nishiguchi, and A. Fujiwara, Appl. Phys. Lett. **94**, 223501 (2009).

[6] G. P. Lansbergen, R. Rahman, C. J. Wellard, I. Woo, J. Caro, N. Collaert, S. Biesemans, G. Klimeck, L. C. L. Hollenberg, and S. Rogge, Nat. Phys. **4**, 656 (2008).

[7] M. Fuechsle, J. A. Miwa, S. Mahapatra, H. Ryu, S. Lee, O. Warschkow, L. C. L. Hollenberg, G. Klimeck, and M. Y. Simmons, Nat. Nanotechnol. **7**, 242 (2012).

[8] B. Roche, E. Dupont-Ferrier, B. Voisin, M. Cobian, X. Jehl, R. Wacquez, M. Vinet, Y.-M. Niquet, and M. Sanquer, Phys. Rev. Lett. **108**, 206812 (2012).

[9] A. L. Efros and B. I. Shklovskii, *Electronic Properties of Doped Semiconductors* (Springer-Verlag, New York, 1984).

[10] G. P. Lansbergen, G. C. Tettamanzi, J. Verduijn, N. Collaert, S. Biesemans, M. Blaauboer, and S. Rogge, Nano Lett. **10**, 455 (2010).

[11] K. A. Matveev and A. I. Larkin, Phys. Rev. B **46**, 15337 (1992).

[12] B. Roche, B. Voisin, X. Jehl, R. Wacquez, M. Sanquer, M. Vinet, V. Deshpande, and B. Previtali, Appl. Phys. Lett. **100**, 032107 (2012).

[13] Y. Taur, IEEE Electron Device Lett. **21**, 245 (2000).

[14] Y. Ono, J.-F. Morizur, K. Nishiguchi, K. Takashina, H. Yamaguchi, K. Hiratsuka, S. Horiguchi, H. Inokawa, and Y. Takahashi, Phys. Rev. B **74**, 235317 (2006).

[15] J. Verduijn, G. C. Tettamanzi, and S. Rogge, Nano Lett. **13**, 1476 (2013).

[16] See Supplemental Material at http://link.aps.org/supplemental/10.1103/PhysRevB.89.161404 for the electric field mapping in the channel in the presence of nearby S-D with graded As donor concentration.

[17] P. P. Altermatt, A. Schenk, and G. Heiser, J. Appl. Phys. **100**, 113714 (2006).

[18] F. A. Mohiyaddin, R. Rahman, R. Kalra, G. Klimeck, L. C. L. Hollenberg, J. J. Pla, A. S. Dzurak, and A. Morello, Nano Lett. **13**, 1903 (2013).

[19] M. Diarra, Y.-M. Niquet, C. Delerue, and G. Allan, Phys. Rev. B **75**, 045301 (2007).

[20] R. Rahman, G. P. Lansbergen, J. Verduijn, G. C. Tettamanzi, S. H. Park, N. Collaert, S. Biesemans, G. Klimeck, L. C. L. Hollenberg, and S. Rogge, Phys. Rev. B **84**, 115428 (2011).

[21] Y. L. Hao, A. P. Djotyan, A. A. Avetisyan, and F. M. Peeters, Phys. Rev. B **80**, 035329 (2009).

[22] M. J. Calderon, J. Verduijn, G. P. Lansbergen, G. C. Tettamanzi, S. Rogge, and B. Koiller, Phys. Rev. B **82**, 075317 (2010).

[23] Y. L. Hao, A. P. Djotyan, A. A. Avetisyan, and F. M. Peeters, J. Phys.: Condens. Matter **23**, 115303 (2011).

[24] M. L. Perrin, C. J. O. Verzijl, C. A. Martin, A. J. Shaikh, R. Eelkema, H. J. van Esch, J. M. van Ruitenbeek, J. M. Thijssen, H. S. J. van der Zant, and D. Dulic, Nat. Nanotechnol. **8**, 282 (2013).